

TECHNICAL REPORT

Variant of Green's Function Nodal Method for Neutron Diffusion

A. TRKOV, M. NAJŽER,

*"J. Stefan" Institute, University of Ljubljana, Yugoslavia**

L. ŠKERGET

*Faculty of Engineering, University of Maribor, Yugoslavia***

Received October 9, 1989

A variant of the Green's function nodal method derived from the boundary integral form of the multigroup neutron diffusion equation in rectangular geometry is presented. As usual in the nodal methods, the multi-dimensional diffusion equation is integrated in the transverse direction. The resulting 1D diffusion equation is solved following the Boundary Element technique in one dimension. In this way a weighted residual method is obtained, with a Green's function for weighting, but with different boundary conditions than normally applied in the Green's function nodal methods. Mathematical formulation of the method is given and the iteration procedure is described. A computer program BINDIF has been designed, based on the new method. Its capabilities include the solution of the multigroup neutron diffusion equation of 1D, 2D and 3D rectangular lattices. The BINDIF program has been checked against other methods used for global reactor calculations on benchmark problems, representative of realistic power reactor cores. The results indicate that the method is attractive to design highly efficient algorithms for a large mainframe, a personal computer or a parallel processor.

KEYWORDS: *neutron diffusion equation, multigroup theory, power distribution, multiplication factors, coarse mesh method, nodal method, Green function, computer codes, computer calculations*

I. INTRODUCTION

The neutron diffusion problem has long been solved to virtually any desired accuracy. Nevertheless there exists an interest in new methods that can offer improved computational efficiency which is essential in applications such as: software for small computers, reactor core simulators and neutronics modules for programs tackling complex transients and core reload optimisation.

Currently the fastest algorithms for solving the diffusion equation are different variants of the Nodal method (reviewed by Dorning⁽¹⁾) whereby the solution in a particular direction is obtained by integrating the diffusion equation in the transverse directions. In this way a multi-dimensional problem is reduced into a

set of one-dimensional problems. The solutions in each direction are coupled through the orthogonal components of the differential operator which appear as an additional neutron source/sink terms in the one-dimensional equations. The performance of a nodal method depends on the efficiency of the algorithm for the solution of the one-dimensional diffusion equation. Several methods have been successfully tried in the past. An approach based on the Boundary Element techniques is described in the present work.

The Boundary Element method was found successful in many fields⁽²⁾ but in a direct application to multi-dimensional neutron diffusion it was found difficult to gain significant

* *Ljubljana, Jamova, 39 JUGOSLAVIA.*

** *Maribor, Smetanova 17, JUGOSLAVIA.*

computational efficiency compared to the Finite Difference and the Finite Element methods, for example. A similar conclusion can be drawn from the work of Itagaki⁽⁸⁾. In one dimension however, integration along boundaries is not required because the boundary integrals reduce to point values of the integrand on the boundaries. The boundary element method reduces to a straightforward boundary solution method⁽⁶⁾ in one dimension. By this approach the diffusion equation is solved for the flux and the current values on the boundaries and no trial functions are required to approximate the neutron flux distribution. Since the boundary conditions can be imposed exactly, the solution is analytical, provided the integrals are calculated with sufficient accuracy. Effectively, a weighted residual method is obtained, where the weighting function is the simplest fundamental solution⁽⁷⁾ to the problem. Of course this is also a Green's function to some particular problem, although its boundary conditions (it goes to infinity as $x \rightarrow \pm\infty$) are physically meaningless. Such Green's function is the consequence of the choice of the weighting function rather than the initial requirement, but the name "Green's function method" is retained for the sake of consistency in nomenclature with other similar methods.

Several methods of solving the one-dimensional diffusion equation using Green's functions have been proposed by other authors. Kobayashi & Nishihara⁽⁶⁾ used the boundary conditions that the Green's function vanishes on the boundaries of homogeneous zones. In this way the neutron current variable disappears from the equations. The unknowns in the system of equations are only the neutron flux values on the boundaries. In designing a nodal method, this approach requires some additional effort in reconstructing the neutron current on the boundaries (and hence the average transverse leakage). Lawrence & Dorning⁽⁴⁾ applied the boundary conditions that the Green's function equivalent of the incoming partial neutron currents vanish on the boundaries of homogeneous zones. In this way the quantities that define the neutron leakage are given

directly from the solution but as a penalty, the number of unknowns increases by a factor of 2.

Compared to other Green's function methods the main advantage of the proposed method is the simplicity of the Green's (weighting) function which allows analytical derivation of some integrals which need to be evaluated, without prohibitive algebraic complexity. The computational efficiency of the new method for one-dimensional neutron diffusion problems has already been confirmed⁽⁸⁾. Coupling the one-dimensional boundary solution technique with the Nodal method produces a new highly efficient multi-dimensional Green's Function Nodal method (BIN) which is described in the present work.

Derivation of equations, general features, iteration strategy and the approximations involved in the new method are described. Results obtained on benchmark problems, representative of realistic power reactor cores are given. Details of the error behaviour, the convergence properties of the method on additional benchmark problems and the effects of different transverse leakage approximations are discussed elsewhere⁽¹⁰⁾.

II. METHOD OF SOLUTION

1. Mathematical Formulation

A multigroup neutron diffusion equation is considered. The system of group diffusion equations is solved by the fission source iteration technique⁽⁸⁾ where initially a fission neutron source distribution is assumed, the equations are solved for each group and from the results the fission neutron source distribution for the next iteration is constructed. For a particular group g the diffusion equation is

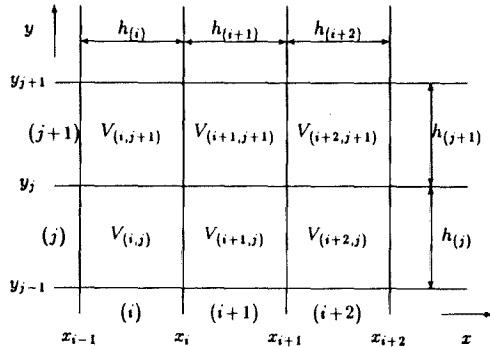
$$-\nabla \cdot D_g \nabla \phi_g + \Sigma_g \phi_g = f_g. \quad (1)$$

The symbols have their usual meaning. The neutron source term f_g is given by

$$f_g = \frac{\lambda_g}{k_{eff}} \sum_n \nu_n \Sigma_{fn} \phi_n + \sum_{h \neq g} \Sigma^{h \rightarrow g} \phi_h. \quad (2)$$

For simplicity consider a two-dimensional array of rectangular homogeneous zones (they may

represent homogenized fuel assemblies). For historical reasons these zones are commonly referred to as *nodes* in the description of the nodal methods. The numbering of the nodes and of the coordinates of their faces are illustrated in **Fig. 1**.



Indices in braces denote intervals and plain indices denote points on a selected coordinate axis.

Fig. 1 Two-dimensional schematic representation of array of nodes illustrating indexation of nodes $V_{(i,j)}$

Consider the node $V_{(i,j)}$. The group diffusion equation in direction x may be written as an integral average in the orthogonal direction y . For clarity the group index g is dropped. Use is made of the Fick's law which relates the neutron flux to neutron current to express the neutron transverse leakage $L_{y(j)}$ in terms of the directional components of the current

$$\begin{aligned} -D_{(i,j)} \frac{d^2 \phi_{x(j)}}{dx^2} + \Sigma_{(i,j)} \phi_{x(j)} \\ = f_{x(j)} - D_{(i,j)} L_{y(j)}, \end{aligned} \quad (3)$$

$$\phi_{x(j)}(x) = \frac{1}{h_{(j)}} \int_{y_{j-1}}^{y_j} \phi(x, y) dy, \quad (4)$$

$$L_{y(j)}(x) = \frac{1}{h_{(j)}} \int_{y_{j-1}}^{y_j} -\frac{\partial^2}{\partial y^2} \phi(x, y) dy, \quad (5)$$

$$= \frac{n_y}{h_{(j)}} \left[\frac{J(x, y_j) - J(x, y_{j-1})}{D_{(i,j)}} \right], \quad (6)$$

$$f_{x(j)}(x) = \frac{1}{h_{(j)}} \int_{y_{j-1}}^{y_j} f(x, y) dy. \quad (7)$$

The solution of the above one-dimensional equation yields the average neutron flux $\phi_{x(j)i}$

and current $J_{x(j)i}$ on the node boundaries i (see Chap. II-2) and from them the *average* leakage in the x direction can be determined

$$\bar{L}_{x(i,j)} = \frac{1}{h_{(i)}} \left[\frac{J_{x(j)i} - J_{x(j)i-1}}{D_{(i,j)}} \right]. \quad (8)$$

This *average* leakage is used to approximate the transverse leakage *distribution* when seeking solution for column (i) of nodes in the (orthogonal) y direction and *vice versa* (see Chap. II-4).

By interchanging the x and the y variables and the corresponding indices, the integral average diffusion equation in the y direction is obtained.

The extension to three dimensions is trivial. To determine the average flux the integration is performed over the two orthogonal directions. Similarly, the transverse leakage is the sum of the leakages in the two orthogonal directions.

2. Solution of One-dimensional Diffusion Equation

The diffusion equation is solved in its weak form which is obtained by a weighted integration of Eq. (3) over a node. The node $V_{(i,j)}$ in row (j) is implied. To simplify the notation the node indices (ij) and the row index (j) are dropped

$$\begin{aligned} \int_{x_{i-1}}^{x_i} \left[-D \frac{d^2 \phi_x}{dx^2} + \Sigma \phi_x \right] w dx \\ = \int_{x_{i-1}}^{x_i} (f_x - D L_y) w dx. \end{aligned} \quad (9)$$

Integrating by parts twice, the differential operator can be transferred from the flux ϕ_x to the weighting function w and the boundary terms. The boundary element technique prescribes the weighting function to be the simplest *fundamental solution*⁽⁷⁾ of the diffusion equation which must satisfy

$$-D \frac{d^2 w}{dx^2} + \Sigma w + D \delta(\xi - x) = 0, \quad (10)$$

where δ is the Dirac delta function. It is zero everywhere except at $(x = \xi)$ where it has a singularity. The integral over the singularity equals *one* by definition. In one-dimensional slab geometry the fundamental solution has

the form :

$$w(\xi, x) = \frac{1}{2\kappa} \sinh(\kappa|\xi - x|), \quad (11)$$

where $\kappa^2 = \Sigma/D$. Note that this is a Green's function to a problem with boundary conditions :

$$w(0) = 0; \quad \lim_{|\xi - x| \rightarrow \infty} w(|\xi - x|) \rightarrow \infty. \quad (12)$$

Such choice of the boundary condition distinguishes the proposed method from other Green's function methods, which are mentioned in the Introduction. The simplicity of the Green's function reduces the effort in preparing the global matrix coefficients and particularly the weighted integrals of the neutron source, defined by Eq. (14), because it allows analytical derivation of the flux expansion coefficients from integral considerations (see Chap. II-3). The results presented in Chap. III indicate that the solution, obtained with the proposed weighting function is not in any way inferior in accuracy compared to the more sophisticated approach.

Substituting expression (11) into Eq. (10), the integrals on the left-hand side reduce to an algebraic expression involving only flux and current average values at ξ and the boundary points x_{i-1} and x_i . An equation

for $\phi_x(\xi)$ is obtained :

$$\begin{aligned} & -D\phi_x(\xi) + J_{x,i} \frac{1}{2\kappa} \sinh \kappa(x_i - \xi) \\ & - J_{x,i-1} \frac{1}{2\kappa} \sinh \kappa(\xi - x_{i-1}) \\ & + \phi_{x,i} \frac{D}{2} \cosh \kappa(x_i - \xi) \\ & + \phi_{x,i-1} \frac{D}{2} \cosh \kappa(\xi - x_{i-1}) \\ & = \frac{1}{2\kappa} \int_{x_{i-1}}^{x_i} [f_x(x') - DL_y(x')] \\ & \quad \cdot \sinh(\kappa|\xi - x'|) dx'. \end{aligned} \quad (13)$$

Note that $J_{x,i}$ and $\phi_{x,i}$ are the neutron current in the x direction and the neutron flux at node boundaries $x = x_i$ averaged over the y -interval of row (j).

Given the values of the flux and the current on the boundaries and also given the neutron source distribution on the right-hand side, the above equation defines *exactly* the neutron flux (averaged over y) at all interior points ξ .

Substituting ξ by the boundary points x_{i-1} and x_i and applying the neutron flux and current continuity across the boundaries, two equations for the node $V_{(i,j)}$ in the x direction are obtained :

$$\begin{bmatrix} \frac{D}{2} \cosh \kappa h & -\frac{1}{2\kappa} \sinh \kappa h & -\frac{D}{2} & 0 \\ -\frac{D}{2} & 0 & \frac{D}{2} \cosh \kappa h & \frac{1}{2\kappa} \sinh \kappa h \end{bmatrix} \cdot \begin{bmatrix} \phi_{i-1} \\ J_{i-1} \\ \phi_i \\ J_i \end{bmatrix} = \begin{bmatrix} F_i \\ F_{i-1} \end{bmatrix},$$

where $F_k = \frac{1}{2\kappa} \int_{x_{i-1}}^{x_i} f(x) \sinh \kappa|x_k - x| dx, \quad (k=i-1, i). \quad (14)$

Assembling such equations for all i in row (j), applying the flux and current continuity conditions on the interfaces and the boundary conditions on the external boundaries, a global matrix for row (j) of nodes is obtained. This matrix is easily converted to tridiagonal form and solved for the average values $\phi_{x(j)i}$ and $J_{x(j)i}$, assuming a given source on the right-hand side. The same can be repeated for all (j). Similarly, the equations for the y direction can be constructed and solved. The

equations are coupled through the transverse leakage which appears in the source term on the right-hand side of Eq. (13).

Note that the left-hand side of Eq. (13) is exact and the accuracy of the method depends entirely on the way in which the integral on the right-hand side is evaluated. No *a priori* assumption is necessary about the functional dependence of the neutron flux. This is the main difference between the currently proposed method and other weighted residual

methods which usually approximate the neutron flux by polynomial trial functions.

For a given source distribution and after solving for the flux and the current values on the node boundaries, Eq. (13) defines the neutron flux (and current) distribution at all interior points. Therefore the neutron source distribution $f(x)$ for the next iteration, which is defined by Eq. (2), can be constructed to any desired accuracy (within the applied transverse leakage distribution approximation). The weighted integrals of the source term, given by Eq. (14) can also be calculated exactly. The procedure is rather tedious, since the flux at every point is defined by an integral. Usually in the Boundary Element method, some sample points are selected at which the flux is calculated. Integration is then performed numerically by the Gauss quadrature rule (or similar). On the other hand, if the neutron source distribution and the transverse leakage are polynomials, then the integral in Eq. (13) can be evaluated analytically. Only for the purpose of evaluating these integrals, the neutron flux distribution and the transverse leakage are approximated by an n -th order Legendre polynomial expansion so that the neutron source distribution in polynomial representation for the next iteration can be constructed.

Both of the above procedures for calculating the integrals have also been applied by Kobayashi & Nishihara⁽⁶⁾. Numerical integration involved the Simpson's rule. The second order flux expansion coefficients were determined from the flux values on the boundaries. The latter approach proved to be computationally much more efficient.

3. Neutron Flux Expansion

For integration purposes the neutron flux in the node $V_{(ij)}$ is expanded in local coordinates in Legendre polynomials $P_i(u)$ with coefficients $g_{(ij)l}$. The local coordinate variable u is obtained by a linear transformation of the interval $[x_{i-1}, x_i]$ into $[-1, 1]$. The Legendre coefficients can be determined by the method of subregions⁽⁶⁾ which is defined by expressions given below and where Eq. (13) is substituted for $\phi_x(\xi)$,

$$\int_{x_a}^{x_b} \phi_x(\xi) d\xi = \frac{h_i}{2} \sum_l g_{(ij)l} \int_{u_a}^{u_b} P_l(u) du. \quad (15)$$

Appropriate integration limits $[x_a, x_b]$ correspond to the following local coordinate intervals $[u_a, u_b]$:

$[-1, 1]$ for the P_0 component

(This is equivalent to the neutron balance condition.)

$[0, 1]$ for the P_1 component

(Together with the P_0 component this guarantees correct average flux over each half-interval.)

$[-\frac{1}{2}, \frac{1}{2}]$ for the P_2 component

$[0, \frac{1}{2}]$ for the P_3 component

(Together with the lower order components this guarantees correct average flux over each quarter-interval.)

The flux and the current values on the boundaries could also be used to determine the Legendre coefficients, but this approach is found to offer considerably less accuracy⁽¹⁰⁾ for the same order of expansion. Coefficients derived by the method of subregions from Eq. (15) are usually preferred, at least for the lower order terms in spite of the more complicated derivation. The same procedure is also applied in the orthogonal directions.

4. Transverse Leakage Treatment

To model the transverse leakage, Finne-*mann et al.*⁽⁹⁾ proposed the *consistent parabolic* approximation where the full continuity of L and $D \cdot dL/dx$ are demanded, and the *linearized* variant which is an approximation to the above. Such a treatment is physically justified when for example 4th order polynomial trial functions are used in flux expansion. The transverse leakage is then a 2nd order polynomial. In the new method currently described there are no assumptions about the flux. In view of other approximations the following simplified, *linear average* approximation seems reasonable. The leakage in the y direction $L_{y(j)i}$ from node $V_{(ij)}$, on the boundary x_i is determined as a linear average of the average

leakages $\bar{L}_{y(i,j)}$ and $\bar{L}_{y(i+1,j)}$ in the neighbouring nodes (i) and ($i+1$) of thickness $h_{(i)}$ and $h_{(i+1)}$, respectively:

$$L_{y(j)i} = \frac{\bar{L}_{y(i,j)}/h_{(i)} + \bar{L}_{y(i+1,j)}/h_{(i+1)}}{1/h_{(i)} + 1/h_{(i+1)}}, \quad (16)$$

and similarly for the orthogonal directions. From the average and the boundary values the Legendre polynomial coefficients of the transverse leakage are determined:

$$L_{y(j)}(u) = \sum_{k=0}^2 l_k P_k(u), \quad (17)$$

$$l_0 = \bar{L}_{y(i,j)}, \quad (18)$$

$$l_1 = \frac{1}{2} [L_{y(j)i} - L_{y(j)i-1}], \quad (19)$$

$$l_2 = \frac{1}{2} [L_{y(j)i} + L_{y(j)i-1}] - l_0, \quad (20)$$

Numerical results have confirmed⁽¹⁰⁾ that there is no loss in accuracy due to a simpler treatment of the transverse leakage. The advantages are a small simplification of the computer code and a slight improvement in efficiency.

5. Inner Iteration Strategy

Usually in the nodal methods the equations are constructed so as to demand iteratively the node-face averaged partial neutron current balance. In the proposed method the node-face averaged flux and *net* current are determined.

Without upscattering and transverse leakage, the fission source distribution from the previous outer iteration is sufficient to solve the system of equations for each group explicitly. The upscattering effects can usually be overcome without additional iterations by using the flux distribution solution from the previous outer iteration to obtain the total neutron source. The transverse leakage distribution approximation is constructed from the average leakage values from a node. These are calculated from the average net currents, which we seek in the solution for a particular energy group. Therefore additional neutron source terms appear on the right-hand side, which depend on the solution. An implicit scheme is obtained which demands iterative solution. These are referred to as the *inner*

iterations. The average leakages from the previous outer iteration are used as an initial guess. Frequently, a single inner iteration is sufficient. An attempt to design an explicit scheme would require a simultaneous solution for all the unknowns within a group, with a matrix of large bandwidth, therefore the iterative scheme is preferred.

With mesh refinement, in the limiting case the transverse leakage is the gradient of the directional component of the neutron current. This is always larger (in absolute value) than the average gradient determined from the average currents on the boundaries of the coarse mesh nodes. On the ultra coarse mesh of the IAEA-2D benchmark problem for example (see Chap. III-1), the maximum transverse leakage source is less than 15% of the total neutron source averaged over the domain of the solution. Convergence of the transverse leakage is faster as compared to the outer iterations and hence a single inner iteration is sufficient. On the other hand for fine meshes (refining the mesh by a factor of 10) the transverse leakage source locally exceeds 85% of the average source. Inner iterations become essential to achieve convergence. Considering the above, the best performance of the method can be expected on ultra-coarse meshes, what is in agreement with the design objectives of the algorithm.

6. Outer Iteration Strategy

The group equations are solved by the usual fission source iteration technique. Outer iteration acceleration optimisation is beyond the scope of the present analysis. The one-parameter cyclic Chebyshev iteration acceleration was applied because it was easy to implement. An iteration cycle consists of K outer iterations. Acceleration is performed on the polynomial expansion coefficients of the fission neutron source. The acceleration parameter $\omega_{k,K}$ for the k -th step of the cycle of length K is

$$\omega_{k,K} = \frac{1}{1 - \frac{1}{2} \left[(b-a) \cos \frac{(2k-1)\pi}{2K} + a+b \right]}, \quad (21)$$

where b is the normalized second-largest eigenvalue of the iteration operator (*i.e.* the dominance ratio) and a the lowest normalized eigenvalue. Variants of the Chebyshev acceleration method differ in the assumptions about a and b . An algorithm such as used in FINELM is adopted; the value ($a=0$) is chosen and the acceleration parameters are sequenced in Lebedev ordering⁽¹¹⁾. For the cases considered the optimal convergence rate was observed for a cycle of length ($K=6$). Longer cycle lengths produced no improvement. The appropriate Lebedev ordering sequence of k values is ($k=2, 5, 3, 4, 1, 6$).

The additional advantage of the selected acceleration scheme is that no additional coefficient vectors need to be stored (as a new coefficient is calculated and extrapolated, the old entry is immediately updated).

For numerical stability reasons the extrapolation of higher order coefficients is switched off in cases where the coefficients change sign between two iterations.

Since the inner iteration are not normally pursued to full convergence, the outer iteration acceleration is also affected. For this reason the acceleration is switched off after each Lebedev cycle until the eigenvalue dominance ratio stabilizes again. The problem is not encountered in one-dimensional cases with no upscattering.

III. RESULTS

A test program BINDIF was coded according to the above description. The test cases were chosen to indicate the performance of the method on realistic problems in comparison to other codes. Results for the following cases are given:

- (1) BSS-11 the two- and three-dimensional IAEA benchmark representative of a typical PWR core from the ANL-7416 Benchmark Problem Book⁽¹²⁾,
- (2) Biblis PWR core benchmark⁽¹⁷⁾ which represents a real operating reactor with "checkboard" fuel loading pattern,
- (3) BSS-13 a 7×7 BWR fuel assembly model from the ANL-7416 Benchmark Problem Book.

The BINDIF solutions were compared against the fine mesh benchmark reference solutions in which the error is assumed to be negligible. In addition, calculations for comparison were performed with a Nodal Expansion code NEXT⁽¹³⁾ and the Finite Element code FINELM⁽¹⁴⁾. Solutions from literature are also quoted. In the following examples BIN_n represents the proposed Green's Function Nodal method with n -th order flux expansion for integration, NEM_n refers to the Nodal Expansion method solution and FEM_n to the Finite Element method solution using n -th order trial functions to approximate the neutron flux.

The selection criteria for the solutions were the minimum central processor execution time (CP) for a solution on the ultra-coarse mesh (one node per assembly/fuel pin), up to 5% error in the local (node averaged) fission source distribution ε_p and 10 pcm error* in the multiplication factor ε_k . The number of outer iterations N_{it} is also considered.

1. BSS-11 2D and 3D IAEA Benchmark

This is perhaps the most widely used benchmark for testing the diffusion codes. Although the geometry and the cross sections are idealized (see **Fig. A1** and **Table A1** in **APPENDIX**) it is representative of a PWR core and provides a reasonable indication of the behaviour of a code in realistic problems.

In **Table 1** the error in k_{eff} , the fission source distribution, the number of iterations and the execution time in comparison with other programs of comparable accuracies are given for the 2D and 3D cases in quadrant ($/4$) or octant ($/8$) geometry on 20 cm mesh. Programs BINDIF, NEXT and FINELM were executed on the VAX-11/750 machine. Their efficiency can be compared directly. The results for other programs are quoted from literature and refer to execution on more powerful machines.

In order to allow some degree of inter-comparison with other programs the 2D and 3D test cases were solved using BINDIF on a variety of machines. The execution times for an octant of the 2D and the 3D cases on

* pcm=parts per 100,000= $10^{-6} k_{eff}$.

Table 1 Comparison of results for IAEA-2D benchmark problem on 20 cm mesh by various codes (Where indicated the quoted results have been taken from the literature.)

Code	Method	Geom.	ε_k (pcm)	$\varepsilon_p^{(a)}$ (%)	N_{it}	CP (s)	Machine
BINDIF	BIN ₃	2D/8	4	1.0	53	8.6	VAX-11/750
BINDIF	BIN ₄	2D/4	4	1.0	51	16.4	VAX-11/750
NEXT	NEM ₅	2D/4	2	1.1	20	31	VAX-11/750
MEDIUM-2	NEM ₅	2D/8	6	1.4	(b)	0.86 ⁽¹⁶⁾	CYBER-175
—	NGFM ^(c)	2D/4	<1	0.7	38	1.8 ⁽¹⁶⁾	CYBER-175
FINELM	FEM ₃	2D/8	<1	0.4	51	1,496	VAX-11/750
BIVAC	FEM ₄	2D/8	9	4.3	(d)	3.4 ⁽¹⁷⁾	IBM-4381
BINDIF	BIN ₃	3D/8	9	1.4	93	446	VAX-11/750
NEXT	NEM ₅	3D/4	7	1.5	24	850	VAX-11/750
—	NGFM ^(c)	3D/4	(e)	0.4	(e)	62 ⁽⁴⁾	CYBER-175

(a) Assembly averaged power in 3D case.

(b) Not available, but on 10 and 3.33 cm mesh⁽¹²⁾ the required number of iterations is 26 and 42, respectively.

(c) Nodal Green's Function Method.

(d) Not available—two parameter acceleration is used.

(e) Not available.

20 cm mesh are presented in **Table 2**.**Table 2** Comparison of CP execution times (s) on various machines for BINDIF solution of octant of IAEA benchmark problem on ultra coarse mesh

Machine	IAEA-2D	IAEA-3D
μ VAX-II	8.6	—
VAX-11/750	8.6	446
VAX-11/780	6.2	336
VAX-8810	1.0	58
CYBER-830	5.6	298
IBM-3090	0.4	23
IBM-PC/XT [†]	184	10,065

[†] With 8087 co-processor, DOS-3.2, MS-FORTRAN 4.0

It has to be emphasized that no effort was made to optimize the coding for machines other than VAX. The same code was compiled with FORTRAN-77 compiler on each machine and executed with default options.

The results indicate that BINDIF is comparable in efficiency to other nodal codes and much faster than the finite element codes. Its CP-time per iteration is favourable but the number of outer iterations indicates that its procedure for accelerating the convergence of outer iterations is inferior to the asymptotic acceleration with coarse mesh rebalancing which is commonly used in other nodal codes.

2. BIBLIS PWR Core

The BIBLIS core is a 2D benchmark which represents a real operating reactor. It has been proposed by Finnemann & Wagner and used by several authors to test the diffusion code capabilities. The geometry and the cross sections are taken from Ref. (17) and are given in **Fig. A1** and **Table A2**.

The results of the BINDIF calculations can be compared against the published values in **Table 3**.

Table 3 Comparison of results for BIBLIS PWR benchmark problem on 23.1226 cm mesh by various codes (Where indicated the quoted results have been taken from the literature.)

Code	Method	Geom.	ε_k (pcm)	ε_p (%)	N_{it}	CP (s)	Machine
BINDIF	BIN ₃	2D/8	3	1.2	71	12.6	VAX-11/750
—	NGFM ^(b)	2D/4	<1	1.7	(d)	1.9 ⁽⁴⁾	CYBER-175
BIVAC	FEM ₄	2D/8	<1	2.4	(c)	4.2 ⁽¹⁷⁾	IBM-4381

(b) Nodal Green's Function method.

(c) Not available—two parameter acceleration is used.

(d) Not available.

Errors in the multiplication factor and the fission source distribution are comparable to those in the IAEA-2D benchmark. The increase in the BINDIF execution time is primarily due to a larger number of outer iterations. Direct comparison of the execution times of the other two codes is not possible because they were run on considerably more powerful machines.

3. BSS-13 BWR Fuel Assembly

The BSS-13 benchmark represents a BWR fuel assembly with homogenized fuel pin cross sections and reflective boundary conditions. The geometry of the problem is shown on **Fig. A2** and **Table A3**. The dimensions of any homogeneous region never exceed 2 cm so this is essentially a fine mesh calculation.

The aim of the exercise is to investigate the efficiency of our method for fine mesh calculations needed to homogenize the fuel assembly cross sections and for calculating the pin power distributions within the assembly.

The neutron fission source distribution was calculated using BINDIF for various orders of the flux expansion and the results are presented in **Table 4**.

Table 4 Comparison of solution parameters for BSS-13 benchmark BWR fuel assembly problem (Reference k_{eff} is about 1.0855)

Method	k_{eff}	ε_p (%)	N_{it}	CP (s)
BIN ₁	1.08569	0.07	64	58
BIN ₂	1.08545	0.05	66	67
BIN ₃	1.08545	0.05	66	79
BIN ₄ †	1.08544	0.10	115	518
BIN ₂ ††	1.08553	0.02	91	288

† No outer iteration acceleration

†† Double mesh density

The exact error in the k_{eff} can not be estimated because the reference solution is only given up to four decimal places. It can be noted that k_{eff} and the neutron fission source distribution are not very sensitive to a decrease in the order of the flux expansion. The execution time however, is considerably longer than in the previous test cases. This

is primarily because inner iterations are now essential due to the fine mesh. A refinement in the inner iteration procedures could enhance the efficiency of the code for this type of problems.

IV. CONCLUSIONS

A variant of the Green's function nodal method is presented with the following key features:

- No *a priori* assumptions about the solution are necessary (polynomial variation on the neutron flux, for example). The 1D solution is analytical except for the approximate integration of the source term.
- The solution parameters are the node face average neutron flux and the net neutron current.
- The algorithm is designed so that a whole row of nodes is solved directly. This enhances the efficiency when the same code is applied to the 1D problems. It also allows easy adaptation of the algorithm for parallel processing.
- A very simple transverse leakage treatment is used which does not add to the overall error.

The results presented indicate that the BIN method is well suited to design algorithms for 1D, 2D and 3D neutron diffusion problems. The currently adopted solution procedure is particularly efficient on ultra-coarse meshes. The advantages of the method are the following:

- The method allows computational efficiency which makes even 3D solutions on a personal computer possible. Very few existing codes exhibit this feature⁽¹⁸⁾.
- The same code can be used to solve 1D, 2D as well as 3D problems with little loss in efficiency on account of generality.
- Good accuracy control is possible by varying the mesh density and the order of the neutron flux expansion for integration.

The fission source iteration technique for determining the k_{eff} in outer iterations has been extensively used and tested in other programs. In comparison with other nodal codes which use the asymptotic acceleration

in combination with coarse mesh rebalancing instead of the Chebyshev acceleration scheme, a significant improvement in computational efficiency seems possible.

An improvement in the inner iteration procedures would allow better performance on the fine mesh calculations and in problems such as the BSS-13 benchmark described in Chap. III-3.

Mild inhomogeneities in the cross section data such as those produced by the burn-up gradients can also be accommodated in the coarse mesh nodal algorithms. This is conveniently achieved by defining a linear spatial dependence coefficient of the absorption cross section such that correct average variation of k_{∞} across the node in each direction is preserved. The additional absorption rate component can be treated as a source term in a similar manner like the transverse leakage.

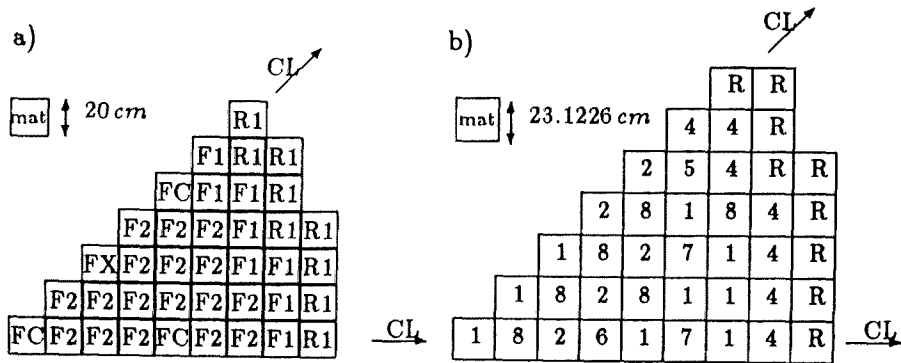
Although the code has not yet been completed to meet the production code standards, it has shown computational efficiency comparable to the fastest nodal codes available. The experience gained with this code can form the basis for designing a highly efficient production code on a large mainframe, a personal computer or a parallel processor.

—REFERENCES—

- (1) DORNING, J.: Modern coarse mesh methods; A development of the '70's, *Proc. Topical Mtg. on Computational Methods in Nucl. Eng., Williamsburg, April 1979*, ANS, Vol. 1, p. 3-2.
- (2) TRKOV, A., NAJŽER, M., ŠKERGET, L., ALUJEVIČ, A.: Boundary element method for neutron diffusion, *Boundary Elements IX*, Vol. 3, (Eds.: BREBBIA, C. A., *et al.*), (1987), Springer-Verlag.
- (3) ITAGAKI, M.: Boundary element method applied to two-dimensional neutron diffusion problems, *J. Nucl. Sci. Technol.*, 22[7], 565~583 (1985).
- (4) LAWRENCE, R. D., DORNING, J.: A nodal Green's function method for multi-dimensional neutron diffusion calculations, *Nucl. Sci. Eng.*, 76, 218~231 (1980).
- (5) KOBAYASHI, K., NISHIHARA, H.: Solution of group-diffusion equation using Green's function, *ibid.*, 28, 93~104 (1967).
- (6) BREBBIA, C. A.: "*The Boundary Element Method for Engineers*", (1978), Pentech Press.
- (7) BATEMAN, H.: "*Partial Differential Equations of Mathematical Physics*", (1959), Cambridge Univ. Press.
- (8) WACHSPRESS, L. E.: "*Iterative Solution of Elliptic Systems*", (1966), Prentice-Hall.
- (9) FINNEMANN, H., BENNEWITZ, F., WAGNER, M. R.: Interface current techniques for multi-dimensional reactor calculations, *Atomkernenergie*, Bd. 30, Lfg. 2, (1977).
- (10) TRKOV, A.: On the boundary element method for the solution of the steady-state neutron diffusion equation, Ph. D. Thesis (in Slovene), Univ. of Maribor, Faculty of Eng., (1989).
- (11) DAVIERWALLA, D. M.: FINELM; A multigroup finite element diffusion code, Part II, R-z, Geometry and numerical accelerations, *EIR-428*, (1981).
- (12) ANL benchmark problem book, *ANL-7416 supplement 2*, (1977).
- (13) KROMAR, M.: Calculation of the power distribution in a power reactor core using the nodal expansion method, M. Sc. Thesis (in Slovene), Univ. of Maribor, Civil Eng. Dept., Yugoslavia, (1987).
- (14) HIGGS, C. E., DAVIERWALLA, D. M.: FINELM; A multigroup finite element diffusion code, Input description, program description and test examples, *EIR-442*, (1981).
- (15) WAGNER, M. R., FINNEMANN, H., KOEBKE, K., WINTER, H. J.: Validation of the nodal expansion method and the depletion program MEDIUM-2 by benchmark calculations and direct comparison with experiment, *Atomkernenergie*, Bd. 30, Lfg. 2, (1977).
- (16) LAWRENCE, R. D., DORNING, J.: A nodal Green's function method for multi-dimensional neutron diffusion calculations, *Trans. Am. Nucl. Soc.*, 28, 248~249 (1978).
- (17) HÉBERT, A.: Application of the Hermite method for finite element reactor calculations, *Nucl. Sci. Eng.*, 91, 34~58 (1985).
- (18) RONACH, A. F.: A Legendre polynomial nodal model for 3D diffusion problems, *Ann. Nucl. Energy*, 14[12], 653~661 (1987).

[APPENDIX] Benchmark Geometry Definitions

(Figs. A1~2, Tables A1~3)



Vacuum boundary conditions are applied on external boundary. Material assignment:

- a) 2D case: Axial buckling is 0.8×10^{-4} . Material FC constitutes location FX.
 3D case: Top slice 20 cm thick consists of R2 at locations FC, FX and material R2 elsewhere.
 Next slice 80 cm thick has material FC at location FX.
 Third slice 260 cm thick has material F2 on location FX.
 Bottom slice 20 cm thick consists entirely of R1.
- b) Geometry of 2D BIBLIS PWR benchmark and material assignment.

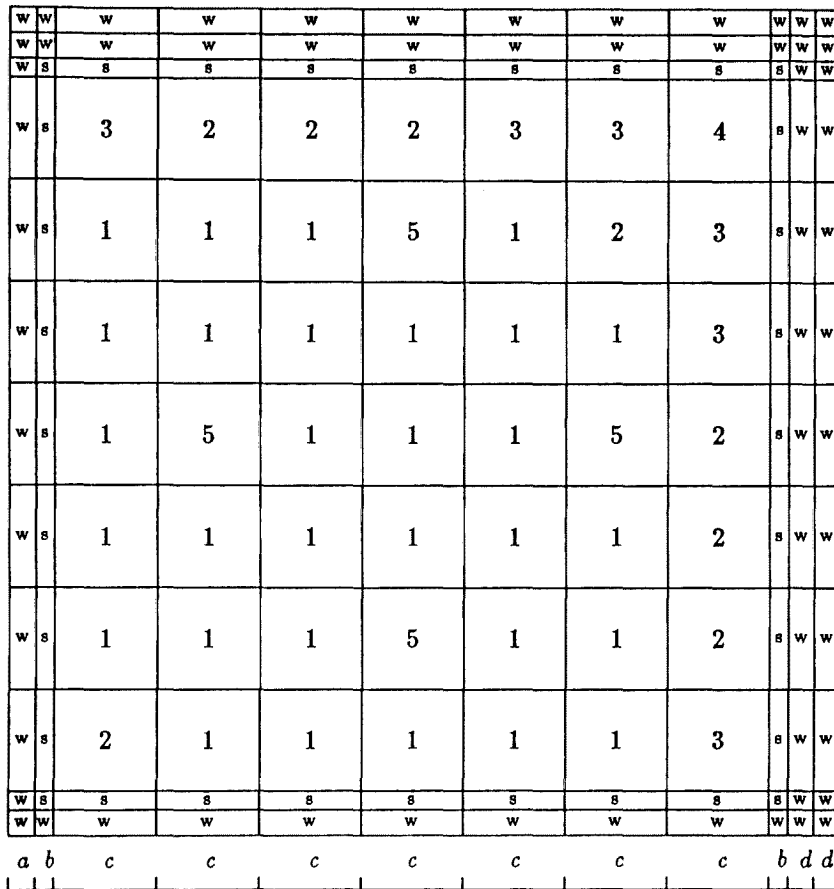
Fig. A1 IAEA benchmark specifications

Table A1 Cross section data for IAEA benchmark problem

Mat.	D_1 (cm)	D_2 (cm)	Σ_{a1} (cm $^{-1}$)	Σ_{a2} (cm $^{-1}$)	$\nu \Sigma_{f2}$ (cm $^{-1}$)	Σ^{1-2} (cm $^{-1}$)
F1	1.5	0.4	0.01	0.080	0.135	0.02
F2	1.5	0.4	0.01	0.085	0.135	0.02
FC	1.5	0.4	0.01	0.130	0.135	0.02
R1	2.0	0.3	0.	0.010	0.	0.04
R2	2.0	0.3	0.	0.055	0.	0.04

Table A2 Cross section data for BIBLIS PWR benchmark problem

Mat.	D_1 (cm)	D_2 (cm)	Σ_{a1} (cm $^{-1}$)	Σ_{a2} (cm $^{-1}$)	$\nu \Sigma_{f1}$ (cm $^{-1}$)	$\nu \Sigma_{f2}$ (cm $^{-1}$)	Σ^{1-2} (cm $^{-1}$)
1	1.4360	0.3635	0.0095042	0.075058	0.0058708	0.096067	0.017754
2	1.4366	0.3636	0.0096785	0.078436	0.0061908	0.103580	0.017621
R	1.3200	0.2772	0.0026562	0.071596	0.0	0.0	0.023106
4	1.4389	0.3638	0.0103630	0.091408	0.0074527	0.132360	0.017101
5	1.4381	0.3665	0.0100030	0.084828	0.0061908	0.103580	0.017290
6	1.4385	0.3665	0.0101320	0.087314	0.0064285	0.109110	0.017192
7	1.4389	0.3679	0.0101650	0.088024	0.0061908	0.103580	0.017125
8	1.4393	0.3680	0.0102940	0.090510	0.0064285	0.109110	0.017027



$$a = 0.47498 \quad b = 0.34544 \quad c = 1.87452 \quad d = 0.47625$$

Numbers 1 to 5 represent fuel cells, S the fuel assembly side wall and W the water gap (dimensions in cm). Reflective boundary conditions are applied on all sides.

Fig. A2 BWR fuel assembly (BSS-13 benchmark) geometry and material assignment

Table A3 Cross section data for BSS-13 BWR fuel assembly benchmark problem

Mat.	D_1 (cm)	D_2 (cm)	Σ_{a1} (cm ⁻¹)	Σ_{a2} (cm ⁻¹)	$\nu\Sigma_{f1}$ (cm ⁻¹)	$\nu\Sigma_{f2}$ (cm ⁻¹)	$\Sigma^{1 \rightarrow 2}$ (cm ⁻¹)
1	1.3170	0.58153	0.008983	0.05892	0.005925	0.09817	0.01069
2	1.3144	0.57800	0.008726	0.05174	0.005242	0.08228	0.01095
3	1.3149	0.57501	0.008587	0.04717	0.004820	0.07200	0.01112
4	1.3160	0.57107	0.008480	0.04140	0.004337	0.05900	0.01113
5	1.3301	0.56951	0.009593	0.16260	0.005605	0.02424	0.01016
S	1.5347	0.70205	0.001043	0.004394	0.	0.	0.009095
W	1.3463	0.29682	0.0001983	0.007796	0.	0.	0.03682